

**Flapping Wing Technology for Micro Air Vehicles  
Incorporating a Lead Zirconate Titanate (PZT) Bimorph  
Actuator**

**by Asha J. Hall, Richard A. Roberts, Isaac Weintraub, and Jaret C. Riddick**

ARL-TR-6040

June 2012

## **NOTICES**

### **Disclaimers**

The findings in this report are not to be construed as an official Department of the Army position unless so designated by other authorized documents.

Citation of manufacturer's or trade names does not constitute an official endorsement or approval of the use thereof.

Destroy this report when it is no longer needed. Do not return it to the originator.

# **Army Research Laboratory**

Aberdeen Proving Ground, MD 21005

---

---

**ARL-TR-6040**

**June 2012**

---

---

## **Flapping Wing Technology for Micro Air Vehicles Incorporating a Lead Zirconate Titanate (PZT) Bimorph Actuator**

**Asha J. Hall and Jaret C. Riddick**

**Vehicle Technology Directorate, U.S. Army Research Laboratory,  
Aberdeen Proving Ground, MD 21005**

**Richard A. Roberts and Isaac Weintraub**

**Air Vehicle Directorate, U.S. Air Force Research Laboratory,  
Wright-Patterson AFB, OH 45433**

<b>REPORT DOCUMENTATION PAGE</b>			<i>Form Approved</i> <b>OMB No. 0704-0188</b>		
Public reporting burden for this collection of information is estimated to average 1 hour per response, including the time for reviewing instructions, searching existing data sources, gathering and maintaining the data needed, and completing and reviewing the collection information. Send comments regarding this burden estimate or any other aspect of this collection of information, including suggestions for reducing the burden, to Department of Defense, Washington Headquarters Services, Directorate for Information Operations and Reports (0704-0188), 1215 Jefferson Davis Highway, Suite 1204, Arlington, VA 22202-4302. Respondents should be aware that notwithstanding any other provision of law, no person shall be subject to any penalty for failing to comply with a collection of information if it does not display a currently valid OMB control number. <b>PLEASE DO NOT RETURN YOUR FORM TO THE ABOVE ADDRESS.</b>					
<b>1. REPORT DATE (DD-MM-YYYY)</b> June 2012		<b>2. REPORT TYPE</b> Final		<b>3. DATES COVERED (From - To)</b> October 2011 to April 2012	
<b>4. TITLE AND SUBTITLE</b> Flapping Wing Technology for Micro Air Vehicles Incorporating a Lead Zirconate Titanate (PZT) Bimorph Actuator			<b>5a. CONTRACT NUMBER</b>		
			<b>5b. GRANT NUMBER</b>		
			<b>5c. PROGRAM ELEMENT NUMBER</b>		
<b>6. AUTHOR(S)</b> Asha J. Hall, Richard A. Roberts, Isaac Weintraub, and Jeret C. Riddick			<b>5d. PROJECT NUMBER</b> TO-VT-01-02		
			<b>5e. TASK NUMBER</b>		
			<b>5f. WORK UNIT NUMBER</b>		
<b>7. PERFORMING ORGANIZATION NAME(S) AND ADDRESS(ES)</b> U.S. Army Research Laboratory ATTN: RDRL-VTM Aberdeen Proving Ground MD 21005			<b>8. PERFORMING ORGANIZATION REPORT NUMBER</b> ARL-TR-6040		
<b>9. SPONSORING/MONITORING AGENCY NAME(S) AND ADDRESS(ES)</b>			<b>10. SPONSOR/MONITOR'S ACRONYM(S)</b>		
			<b>11. SPONSOR/MONITOR'S REPORT NUMBER(S)</b>		
<b>12. DISTRIBUTION/AVAILABILITY STATEMENT</b> Approved for public release; distribution unlimited.					
<b>13. SUPPLEMENTARY NOTES</b>					
<b>14. ABSTRACT</b> Army operations have placed a high premium on reconnaissance missions for unmanned aerial vehicles (UAVs) and micro air vehicles (MAVs) (15 cm or less in dimension and less than 20 g in mass). One approach for accomplishing this mission is to develop a biologically inspired flapping wing insect-sized device that can maneuver into confined areas. Analysis of insect flight indicates that in addition to the bending excitation (flapping), simultaneous excitation of the twisting degree of freedom (pitching) is required to adequately control the vehicle. Traditionally, bimorph piezoelectric lead zirconate titanate (PZT) ( $\text{Pb}(\text{Zr}_{0.55}\text{Ti}_{0.45})\text{O}_3$ ) actuators have been used to excite the bending degree of freedom. In laminated or layered structures, bend-twist coupling is governed by having at least one anisotropic layer not aligned with the primary plate axes. By adding a layer of off-axis PZT segments to a PZT bimorph actuator, a functionally modified bimorph now offers a bend-twist coupling, flexural response in the traditional bimorph actuator. This study presents an experimental investigation of both traditional bimorph and functionally modified PZT bimorph designs intended for active bend-twist actuation of cm-scale flapping wing devices. Results are shown comparing aerodynamic parameters for three wing shapes and two PZT designs.					
<b>15. SUBJECT TERMS</b> piezoelectric bimorph actuator, flapping wing, micro air vehicle					
<b>16. SECURITY CLASSIFICATION OF:</b>			<b>17. LIMITATION OF ABSTRACT</b> UU	<b>18. NUMBER OF PAGES</b> 20	<b>19a. NAME OF RESPONSIBLE PERSON</b> Asha J. Hall
<b>a. REPORT</b> Unclassified	<b>b. ABSTRACT</b> Unclassified	<b>c. THIS PAGE</b> Unclassified			<b>19b. TELEPHONE NUMBER (Include area code)</b> (410) 278-8036

Standard Form 298 (Rev. 8/98)  
Prescribed by ANSI Std. Z39.18

---

## Contents

---

<b>List of Figures</b>	<b>iv</b>
<b>List of Tables</b>	<b>iv</b>
<b>1. Introduction</b>	<b>1</b>
<b>2. Experimental</b>	<b>3</b>
<b>3 Results and Discussion</b>	<b>5</b>
3.1 Displacement versus Frequency .....	5
3.2 Selection of Venation Pattern.....	6
3.3 Lift Forces .....	8
<b>4. Conclusion</b>	<b>11</b>
<b>5. References</b>	<b>12</b>
<b>Distribution List</b>	<b>14</b>

---

## List of Figures

---

Figure 1. (a) Three-dimensional (3-D) view of bimorph actuator and (b) side view of bimorph. ....	2
Figure 2. Mechanical amplification scheme. ....	2
Figure 3. Mechanical amplification scheme (a) diagram and (b) picture. ....	2
Figure 4. (a) Three-dimensional view of FMB actuator and (b) side view of FMB actuator. ....	3
Figure 5. Nano-17 6-axis force/torque transducer. ....	4
Figure 6. Net digital board and nano 17-R transducer. ....	4
Figure 7. Displacement as a function of frequency measured at $\pm 36V_{pp}$ for the functionally modified bimorph. ....	6
Figure 8. Axial air velocity below the flapping wing. ....	6
Figure 9. Batten structure of (a) Wing 1, (b) Wing 2, and (c) Wing 3. The batten structure was formed on a 3-D prototyping machine and the membrane (wing skin) made of low density polyethylene was attached subsequently with an adhesive. ....	7
Figure 10. Lift measurements for the traditional bimorph with Wing Type 1 design. ....	7
Figure 11. Lift measurements for the traditional bimorph with Wing Type 2 design. ....	7
Figure 12. Lift measurements for the traditional bimorph with Wing Type 3 design. ....	8
Figure 13. FMB actuator average lift of 10 mN with Wing Type 1 design. ....	9
Figure 14. High-speed camera image depicting asymmetric flapping: (a) front view and (b) top view. ....	10
Figure 15. Traditional bimorph actuator vs. FMB actuator displacement. ....	10

---

## List of Tables

---

Table 1. Comparison of lift results and wing design. ....	8
---	---

---

## 1. Introduction

---

Unmanned aerial vehicles (UAVs) and micro air vehicles (MAVs) provide situational awareness that shapes the decisions of the squad command. As such, these platforms are designed to serve as “eyes and ears” for the Soldier. One approach for accomplishing this mission is to develop a biologically inspired flapping wing insect that can maneuver into confined areas and hover, while obtaining data undetected. In order to execute aerial maneuvers, insects must not only generate lift to remain aloft, but they must also manipulate aerodynamic forces to steer and maneuver (1). For example, during flight, fruit flies ride on top of their vortices; this, in turn, creates lift. Analysis of insect flight indicates that in addition to the bending excitation (flapping), a simultaneous excitation of the twisting degree-of-freedom (pitching) is required to manipulate the control surface adequately (2). The focus of this report is to demonstrate the ability of a lead zirconate titanate (PZT) actuator to function as the driving mechanism for a flapping wing platform. The goal is to compare and discuss the flapping amplitude and resultant lift of the flapping excitation for four different flapping wing vehicles.

Traditionally, PZT bimorph actuators have been used in many applications to excite the bending degree of freedom (DOF) (2). A common bimorph configuration consists of two thin ceramic plates bonded together and driven with opposing electrical fields. One plate expands while the other contracts, resulting in a bending deflection of the bimorph construction.

Piezoelectric actuators operate under the reverse piezoelectric effect, wherein an electrical current passes through the material and it undergoes strain (up to 4%). Since the piezoelectric strain is not significant enough to generate a large deflection, a mechanical amplification scheme is needed to generate a considerable amount of displacement. As shown in figure 1, a piezoelectric bimorph is constructed from bonding two plates of piezoelectric materials so that their polarizations are anti-parallel to one another when an electric field is applied across the beam. In this way, the piezoelectric bimorph creates a bending moment, one layer expands while the other layer contracts. As shown in figure 2, a 3-cm PZT-5H bimorph actuator oscillating at resonance frequency is coupled to a flexural wing placed at the distal end of the bimorph. Figure 3 shows in greater detail the mechanical amplification scheme developed to further increase the bending excitation of the bimorph actuator. The motion of the PZT drives a lever mechanism attached to the wing root, which amplifies the wing stroke. As a result, a flapping motion is generated from operating at the fundamental resonance frequency of the system. It has been demonstrated that this simple actuation mechanism delivers one DOF. Michelson et al. (3) stated in his biologically inspired insect flight study that simply being able to beat wings is not adequate enough to sustain hovering flight; one must be able to develop the power necessary to fly.

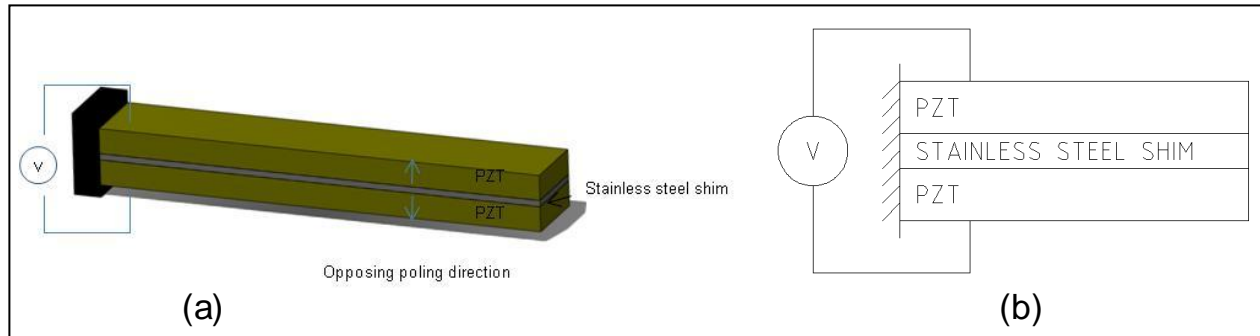


Figure 1. (a) Three-dimensional (3-D) view of bimorph actuator (b) side view of bimorph.

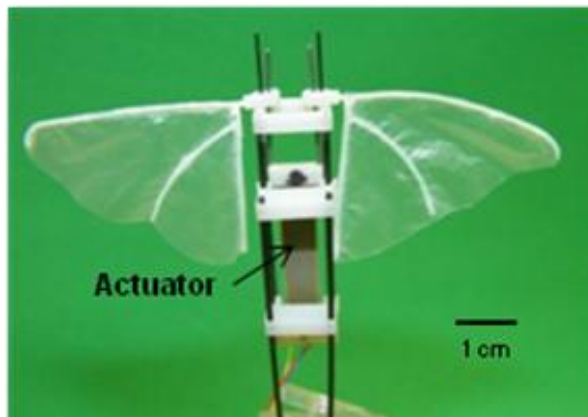


Figure 2. Mechanical amplification scheme.

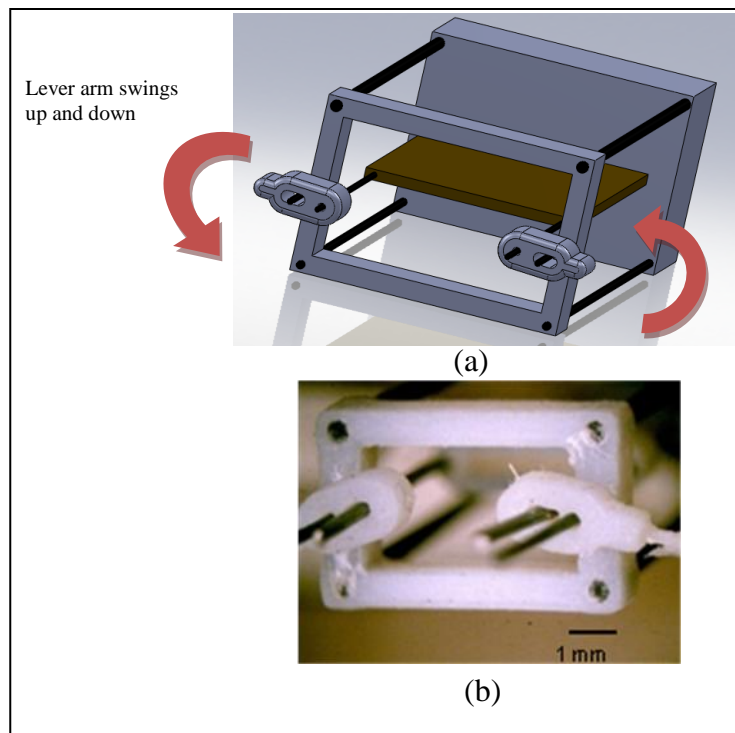


Figure 3. Mechanical amplification scheme (a) diagram and (b) picture.

In order to augment simple wing beats, a laminated or layered actuator structure is created using PZT segments that are not aligned with the primary plate axes (5). This approach is shown in figure 4, where bend-twist coupling is introduced to the flexural response of the layered PZT by adding off-axis PZT segments active in shear, thereby producing a layered structure, a functionally modified bimorph (FMB). Furthermore, by selectively charging off-axis layers in specific combinations with the bimorph, the response of the FMB may be tailored to yield a biaxial actuator that can actively control the flapping wing response.

Most flying insects have three DOFs: wing angle, angle of attack, and out of stroke plane deviation (4). In order to achieve sufficient lift, there are four mechanisms—translational lift, circulatory lift, non-circulator lift, and wake capture—that are employed to generate lift forces (5). Hence, a functionally modified piezoelectric bimorph has been designed to realize two DOFs of motion, namely, the flapping and twisting motions, facilitated by a simple actuation mechanism. The aim of this approach is to demonstrate that it is possible to obtain a flapping motion by coupling a polymeric wing to a distal end of a piezoelectric bimorph actuator, replacing the use of motors. In this report, one DOF of motion, specifically the bending motion, is addressed and the translation of the passive pitching motion of the wings is assessed.

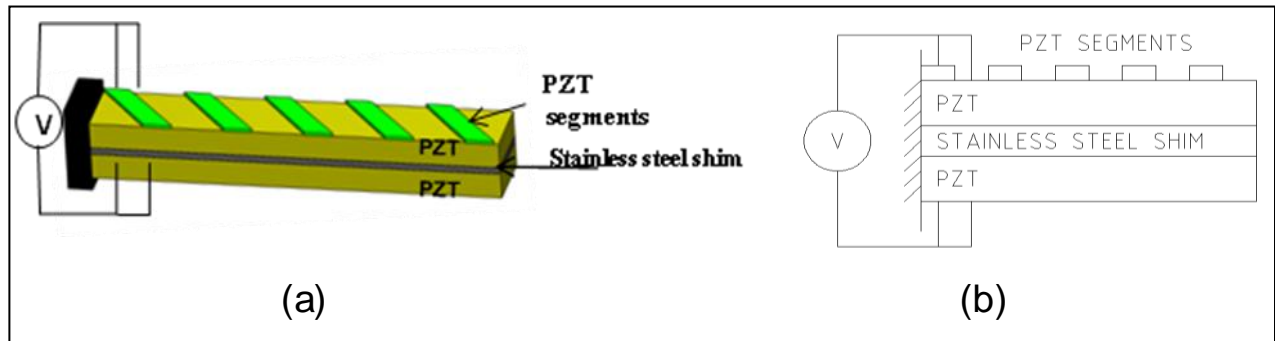


Figure 4. (a) Three-dimensional view of FMB actuator and (b) side view of FMB actuator.

## 2. Experimental

PZT bimorphs were purchased from Physik Instrumente L.P., USA, and the dimensions were 3.6 cm in length, 0.65 cm in width, and 0.075 cm in thickness. Three types of wings were fabricated with low density polyethylene, Fullcure®930, and electro active polymer dimethylsiloxane. The relative thickness of each type of wing material was 20  $\mu\text{m}$  thick for the low density polyethylene. The polymeric wing spars were made of FullCure®840 Veroblue produced from an Eden 260V 3-D printer manufactured by Objet Geometries Ltd. The peak to peak displacement was measured using a MTI-2100 Fotonic™ Sensor manufactured from MTI Instruments (6). The flapping wing wind speed was measured with a hot wire thermo

anemometer by Extech Instruments Inc., which measures airflow down to 40 ft/min (0.45 mi/h) with a basic accuracy  $\pm 3\%$ .

The lift measurements were taken with a Nano-17 force torque transducer manufactured by ATI Industrial Automation. This sensor is an extremely small (17 mm diameter), 6-axis transducer typically used in robotics applications. As shown in figure 5, the Nano-17 is composed of internal silicon strain gauges within the transducer. The analog inputs are sent to a Net F/T box manufactured by ATI. Signals are then filtered and converted to digital signals and transmitted to a computer via Ethernet. The computer is capable of buffering the measurements and storing the counts to a text file which was later parsed using MATLAB (figure 6).

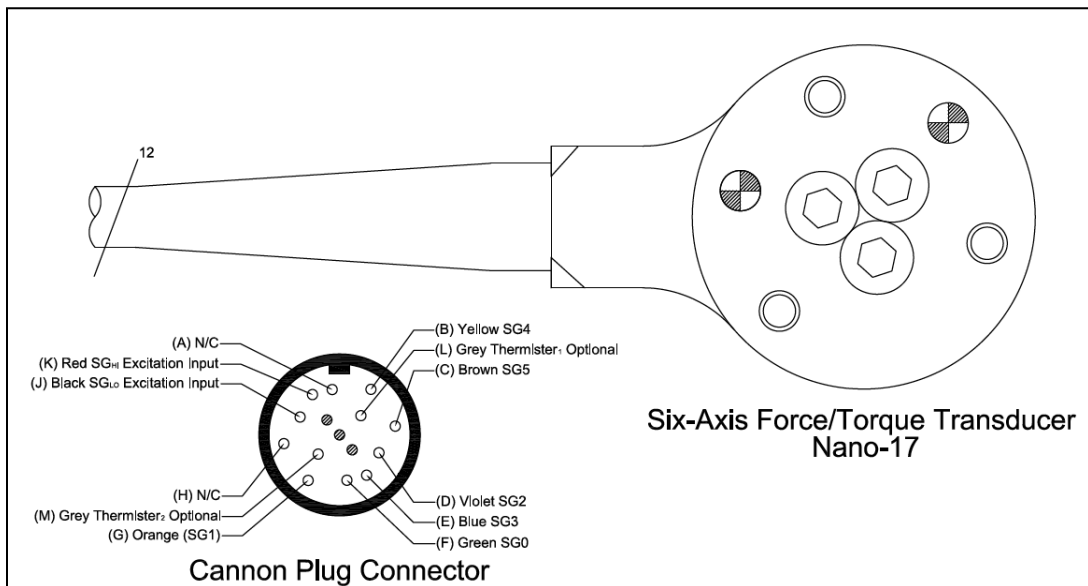


Figure 5. Nano-17 6-axis force/torque transducer.

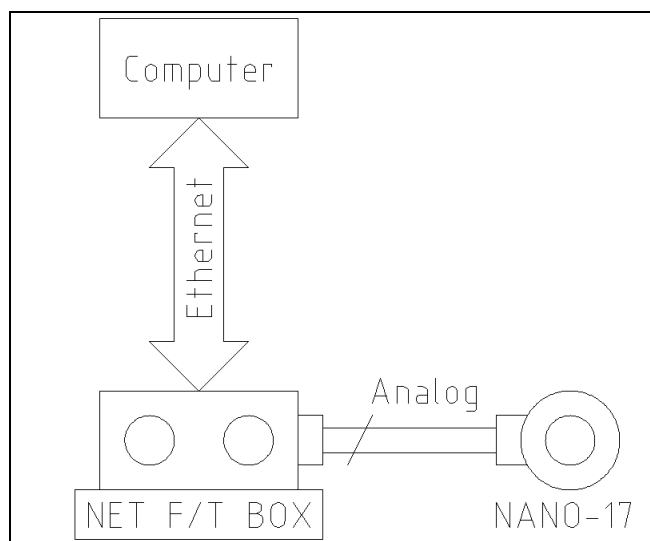


Figure 6. Net digital board and nano 17-R transducer.

The sensor used was calibrated to a maximum axial load of 4.25 lbs-force (18.9N), much higher than seen during testing. It has a resolution of 0.354 grams-force. In order to reduce the effect of environmental vibration, the sensor was attached to a Thor Labs optical table. The high mass and damping available assisted in reducing noise from the environment.

---

### **3 Results and Discussion**

---

#### **3.1 Displacement versus Frequency**

Figure 7 shows the flapping wing tip displacement as a function of flapping frequency. Both the traditional bimorph actuator and the FMB actuator are made of PZT-5H. The displacement measurements were taken from a 22- $\mu\text{m}$ -thick, low density polyethylene wing with a Wing Type 1 design (the wing is later shown in figure 10). The maximum flapping wing tip amplitude measured at 11 mm while operating at 21-Hz resonance frequency at  $\pm 36\text{V}$ . As shown in figure 7, it was confirmed that operating at the resonance frequency yields the highest displacement. Figure 8 displays the average axial air velocity produced by the low density polyethylene flapping wing obtained by using an Extech anemometer. Measurements were obtained at 21 Hz averaged over 400 s. The distance between the trailing edge of the wing and the anemometer was maintained at 1 mm for all measurements. The maximum flow produced by the wings was measured to be 1117.6 mm/s at resonance (21 Hz). The spar motion, the bimorph amplification scheme, and the mechanical transmission element are all parameters that dictate the total flapping amplitude. It has been concluded that there is a direct relationship between the wing flapping amplitude and the air velocity over the range tested when the device is operated at the fundamental resonance frequency of the system. It should be noted that the flapping wing orientation of figure 8 pushes the wind down serving to lift the actuator-wing system. Insect flight of the mesoscale (1–15 cm range) lifts the insect in and out of the wing plane direction and is achieved by a combination of large stroke amplitude and wing rotation.

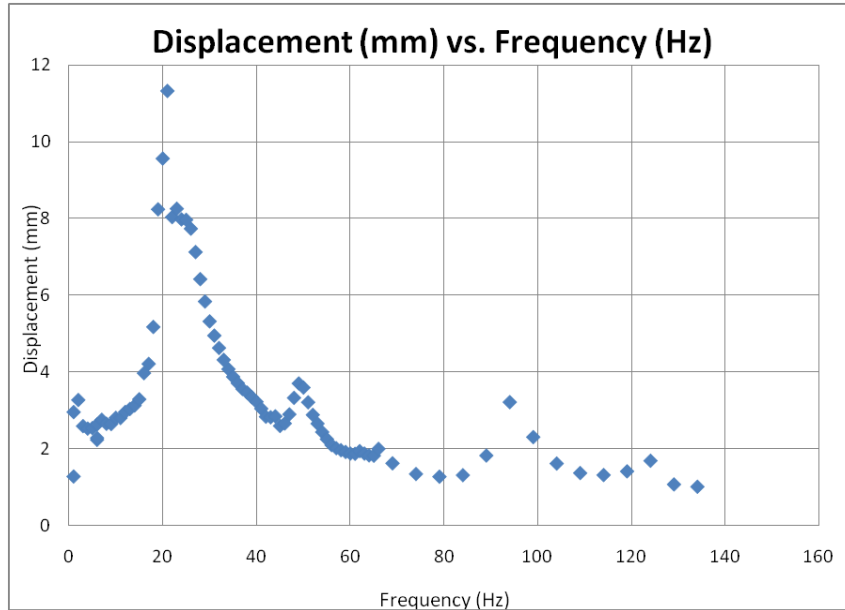


Figure 7. Displacement as a function of frequency measured at  $\pm 36V_{pp}$  for the functionally modified bimorph.

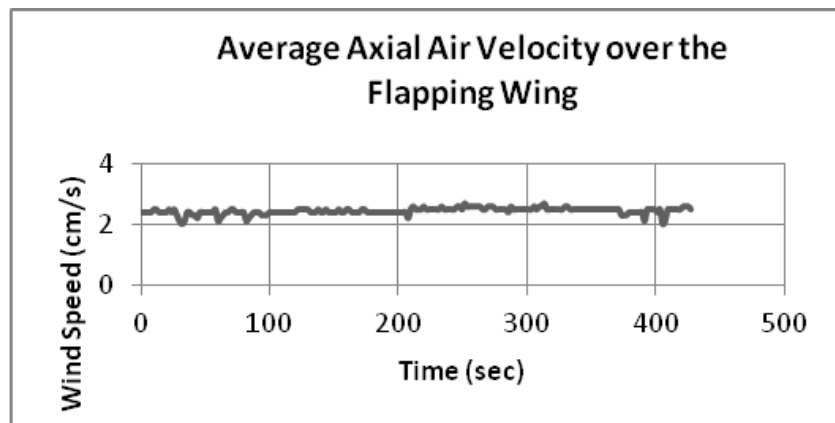


Figure 8. Axial air velocity below the flapping wing.

### 3.2 Selection of Venation Pattern

Instantaneous forces on the wings change during a stroke cycle due to the turning of the wings, deformability of joints, attack angle, rotary velocity of the wings, elastic properties, or flight velocity. All three wing designs have the same wing membrane thickness of  $20 \mu\text{m}$ . All three batten structures were fabricated on an Eden 260V 3-D prototyping machine, as shown in figure 9. The membrane (i.e., wing skin) is made of low density polyethylene plastic and is subsequently attached with an adhesive after the 3-D deposition is completed. The wings are of the same centimeter length with a variation in the geometry and the batten structure, as shown in figures 10 through 12. A comparison in lift measurements were taken and discussed in section 3.3.

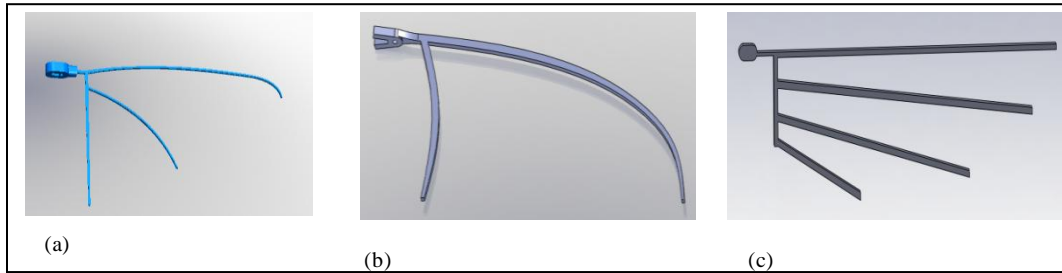


Figure 9. Batten structure of (a) Wing 1, (b) Wing 2, and (c) Wing 3. The batten structure was formed on a 3-D prototyping machine and the membrane (wing skin) made of low density polyethylene was attached subsequently with an adhesive.

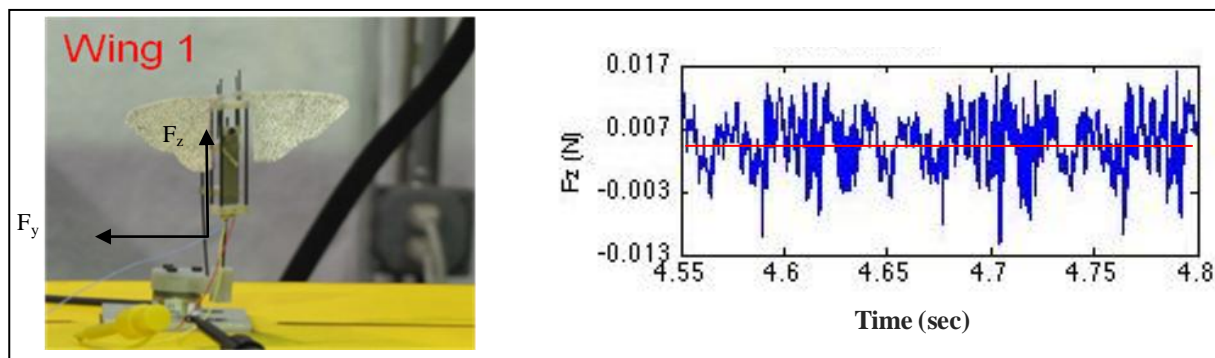


Figure 10. Lift measurements for the traditional bimorph with Wing Type 1 design.

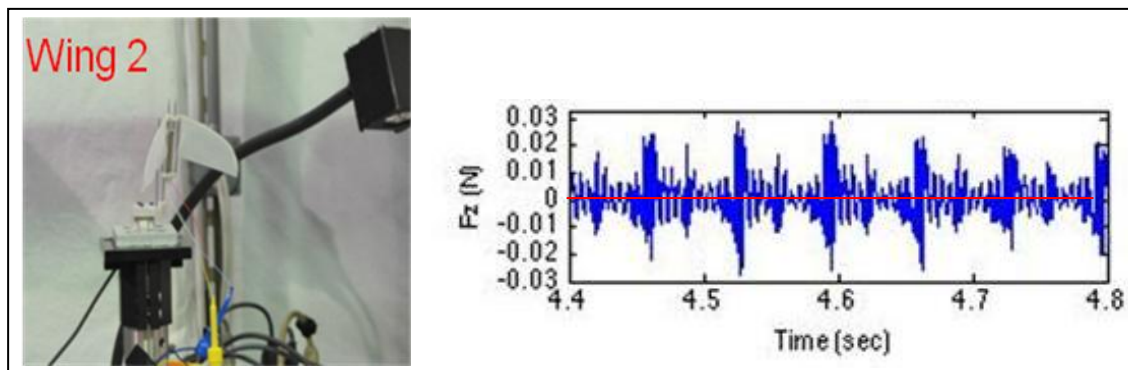


Figure 11. Lift measurements for the traditional bimorph with Wing Type 2 design.

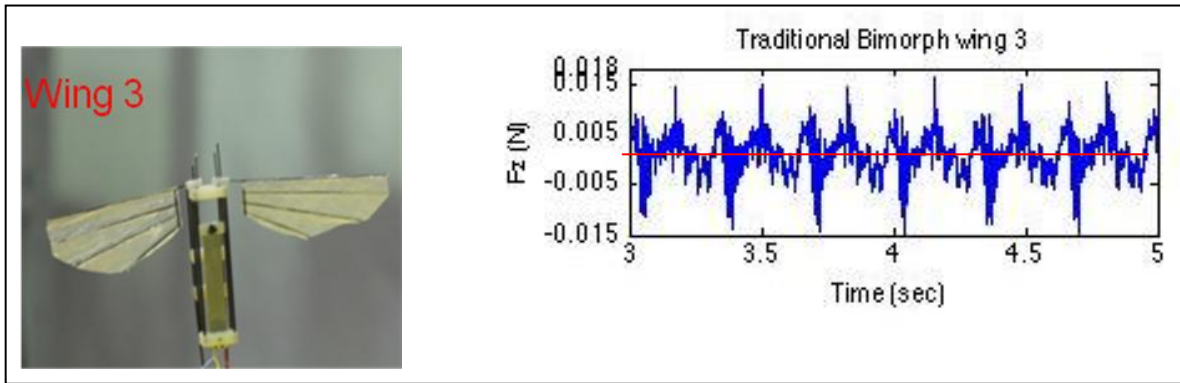


Figure 12. Lift measurements for the traditional bimorph with Wing Type 3 design.

### 3.3 Lift Forces

Stroke amplitude, wing angle of attack, wing tip trajectory, wing beat frequency, and wing rotation are all flapping kinematic characteristics that are required to produce lift. The flapping motion is amplified by a mechanical amplification scheme driven by a piezoelectric actuator resulting in a  $45^\circ$  flap angle response from the wing. The resultant lift force experienced by the flexible wings is shown in figures 10 through 12. The horizontal lift is the useful propulsive force otherwise known as the down stroke sweep direction, which is taken as positive force. The high-speed camera images confirm a  $45^\circ$  angle of attack formed by passive wing rotation, enabling the formation of lift augmentation thereby creating lift. As shown in figure 10, using the traditional bimorph 4-mN upstroke of force is generated by a flexible Wing Type 1 design operated at a 21-Hz flapping frequency. Table 1 gives the comparisons of each wing design and their respective lift values.

Table 1. Comparison of lift results and wing design.

Wing Design	Average Lift	Bimorph Type
Wing Type 1	4 mN	Traditional Bimorph
Wing Type 2	0 mN	Traditional Bimorph
Wing Type 3	2mN	Traditional Bimorph
Wing Type 1	10 mN	Functionally Modified Bimorph

A positive lift peak represents a rotation at the end of a stroke reversal. If there is a delay in rotation, negative lift results at the beginning of the half stroke (5). In the Wing Type 1 case, there seems to be a delay in rotation, yielding an increase in negative lift. At the same flapping frequency, different wing structures generate different lift values. For example, in figure 11, Wing Type 2 displays an average force of zero and validates that the wing design could not produce a significant amount of aerodynamic lift force during the stroke. The design of Wing Type 2 does not have battens or reinforcements in the span direction, resulting in the least wing rotation of all the wing designs presented. Figure 12 depicts Wing Type 3, wherein the lift shows slightly improved average results. Wing Type 3 has venation patterns divided into a number of

span-wise strips that can rotate independently about the longitudinal axis of the wing. The resultant forces on this wing type did not show a significant improvement. However, as shown in figure 13, the FMB actuator was combined with Wing Type 1 and yielded the highest lift during the test period (10 mN). In this experiment, asymmetric flapping is captured by the high-speed cameras, which aid in the understanding of the flapping motion (figure 14). There is a higher wing tip displacement generated by the FMB actuator in comparison to the traditional bimorph actuator, as shown in figure 15. This could contribute to the fundamental understanding validating an increased value in lift for the FMB actuator. The increased mass loading on the tip end of the FMB actuator increases the bending moment translating into an increased displacement

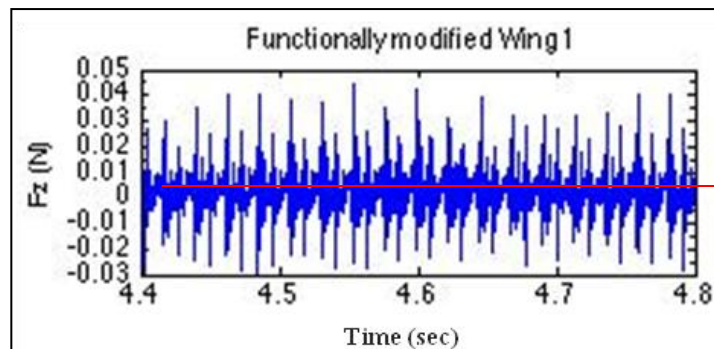


Figure 13. FMB actuator average lift of 10 mN with Wing Type 1 design.

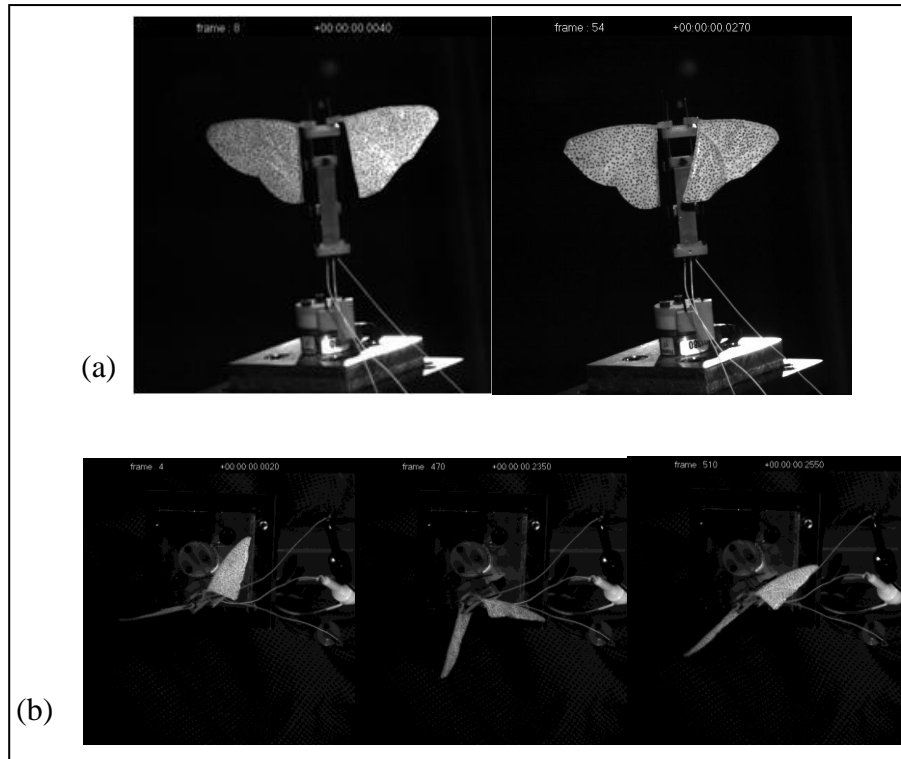


Figure 14. High-speed camera image depicting asymmetric flapping: (a) front view and (b) top view.

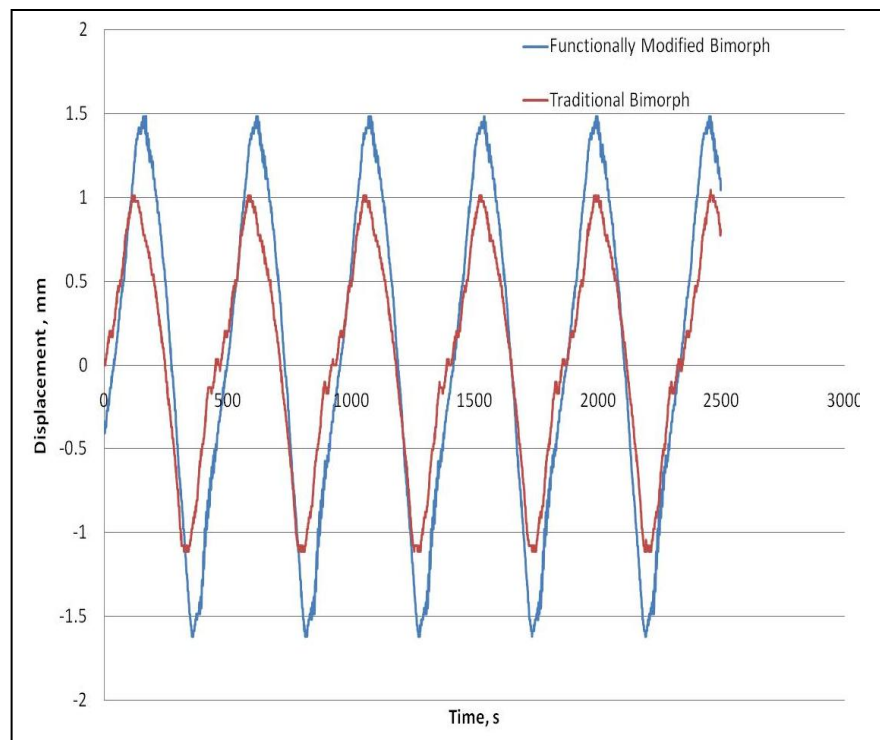


Figure 15. Traditional bimorph actuator vs. FMB actuator displacement.

---

## 4. Conclusion

---

A functionally modified piezoelectric bimorph was designed to realize one DOF of motion, namely, the flapping, facilitated by a simple actuation mechanism. Experimental results indicated that at resonance the maximum peak-to-peak displacement measurements of the FMB exceed measurements for the traditional bimorph. We have demonstrated 11-mm deflection of one DOF of flapping motion with flapping wing wind speeds of 2.5 cm/s. The FMB actuator combined with Wing Type 1 yielded the highest lift, 10 mN, or 1.1212 gram-force on a 2.5 gram-force vehicle (minus the circuit board). This is attributed to the increase in flapping angle shown in figure 13. This result contributes to our fundamental understanding, validating an increased value in lift for the FMB actuator. The increased mass loading on the tip of the FMB actuator increases the bending moment, therefore, translating into an increased displacement.

The preliminary lift results indicate that more work needs to be done to increase the lift of the system to at least the weight of the vehicle. Future work will include numerical validation of the 3-D bending analysis via finite-element analysis and experimental validation, with the ultimate goal of developing a design tool for biaxial actuators for cm-scale flapping wing MAVs.

---

## 5. References

---

1. Dickinson, M.; Lehmann, F.-O.; Sane, S. P. Wing Rotation and the Aerodynamic Basis of Insect Flight. *Science* **1999**, *284*, 1954–1960.
2. Mueller, T. J. Fixed and Flapping Wing for Micro Air Vehicles, American Institute of Aeronautics and Astronautics, V195, 2001, Massachusetts, USA.
3. Michelson, R. C.; Reece, S. Update on Flapping Wing Micro Air Vehicle Research. *13<sup>th</sup> Bristol International RPV Conference Proceedings*, 30 March–1 April 1998.
4. Yan, J.; Wood, R. J.; Avadhanula, S.; Sitti, M.; Fear, R. S. Towards Flapping Wing Control for a Micromechanical Flying Insect. *Proceedings of the 2001 International IEEE conference on Robotics and Automation*, Seoul Korea, 2001, 3901–3908.
5. Agrawal, A.; Agrawal, S. K. Design of Bio-Inspired Flexible Wings for Flapping Wing Micro-sized Air Vehicle Applications. *Advanced Robotics* **2009**, *23*, 979–1002.
6. Hall, A.; Bundy, M. *Overview of Piezoelectric Actuator Displacement Measurements Utilizing a MTI-2100 Fotonic Sensor*; ARL-TN-0429; U.S. Army Research Laboratory: White Sands Missile Range, NM, April 2011.
7. Wang, J. Z. Dissecting Insect Flight. *Annual Review Fluid Mechanics* **2005**, *37*, 183–210.
8. Wu, P.; Stanford, B.; Ifju, P. Passive Bending and Twisting Motion during the Flapping Stroke of a Micro Elastic Wing for Thrust Production. *Proceedings of the 47<sup>th</sup> American Institute of Aeronautics and Astronautics Aerospace Sciences Meeting*, 2009, Orlando FL, 1–17.
9. Wang, Qing Ming; Cross, L. Eric. Performance Analysis of Piezoelectric Cantilever Bending Actuators. *Ferroelectrics* **1998**, *215*, 187–213.
10. Wetherhold, R. C.; Aldraheim, O. J. Bending and Twisting Vibration Control of Flexible Structures Using Piezoelectric Materials. *Shock and Vib. Dig.* **2001**, *33* (3), 187–197.
11. Crawley, E. F.; de Luis, J. Use of Piezoelectric Actuators as Elements of Intelligent Structures. *AIAA J.* **1987**, *25* (10) 1373–1385.
12. Aldraheim, O. J.; Wetherhold, R. C. Mechanics and Control of Coupled Bending and Twisting Vibration of Laminated Beams. *Smart Mtls. and Struct.* **1997**, *6*, 123–133.
13. Park, C.; Walz, C.; Chopra, I. Bending and Torsion Models of Beams with Induced-Strain Actuators. *Smart Mtls. and Struct.* **1996**, *5*, 98–113.

14. Ballato, A.; Kim, Y. Displacements and Rotations of Practical Vibrational Modes of Piezoelectric Bimorph Cantilever Beams. *Proceedings of First IEEE International Conference on Sensors*, Orlando, FL, June 12–14, 2002, 2, 1294–1297.
15. Smits, J. G.; Dalke, S. I.; Cooney, T. K. The Constituent Equations of Piezoelectric Bimorphs. *Sens. and Act. A* **1991** 28, 41–61.
16. Bauchau, O. A.; Craig, J. I. *Structural Analysis: With Applications to Aerospace Structures*; Springer: Dordrecht, Heidelberg, London & New York, 2009, 171–202.
17. Wolfram, S. *The Mathematica Book*; Wolfram Media/Cambridge University Press: Champaign, Cambridge, New York, and Melbourne, 1999.

1 DEFENSE TECHNICAL  
(PDF INFORMATION CTR  
only) DTIC OCA  
8725 JOHN J KINGMAN RD  
STE 0944  
FORT BELVOIR VA 22060-6218

1 DIRECTOR  
US ARMY RESEARCH LAB  
IMNE ALC HRR  
2800 POWDER MILL RD  
ADELPHI MD 20783-1197

1 DIRECTOR  
US ARMY RESEARCH LAB  
RDRL CIO LL  
2800 POWDER MILL RD  
ADELPHI MD 20783-1197

1 DIRECTOR  
US ARMY RESEARCH LAB  
RDRL CIO LT  
2800 POWDER MILL RD  
ADELPHI MD 20783-1197

ABERDEEN PROVING GROUND

3 US ARMY RESEARCH LAB  
ATTN RDRL VTM  
A HALL  
J C RIDDICK  
M BUNDY  
4603 FLARE LOOP  
APG MD 21005

2 US AIR FORCE RESEARCH LAB  
ATTN AFRL/RBAL  
R ROBERTS  
I WEINTRAUB  
2145 FIFTH ST. ROOM 220  
WRIGHT-PATTERSON AFB, OH 45433